

RESEARCH

Eco-friendly treatment of textile dye from aqueous solution using encapsulated biosorbent matrix beads: kinetics and breakthrough analysis

Radhakrishnan Kannan¹ · Sethuraman Lakshmi¹ · Natarajan Aparna¹ · Sivaraman Prabhakar² · Wilson Richard Thilagaraj¹

Received: 3 July 2015 / Accepted: 8 June 2016 / Published online: 17 June 2016
© The Author(s) 2016. This article is published with open access at Springerlink.com

Abstract In this study, *Moringa oleifera*-encapsulated alginate beads (MEA) were synthesized using Ca-alginate for the removal of anionic blue-FFS (AB-FFS) dye from an aqueous solution. The synthesized beads were characterized by scanning electron microscopy (SEM), Fourier transform infrared spectroscopy (FT-IR) and Brunauer–Emmett–Teller (BET) methods. The influences of initial pH, initial dye concentration and temperature were established in batch mode. The equilibrium biosorption obeyed both the Langmuir and Freundlich isotherm models with Q_{\max} of MEA of about 76.92 mg/g at 343 K. Based on thermodynamic data, it was found that the biosorption process was endothermic and spontaneous. Fixed bed column studies were conducted using different parameters such as flow rate and bed height of the biosorbent. The data obtained were fitted with well-established models, namely Thomas and Yoon–Nelson. Desorption of beads could be achieved by a minimum of five successive cycles without significant loss of initial dye concentration in the batch mode. Experimental results indicate that MEA appears to be a promising biosorbent material used for treating the textile wastewater.

Keywords Breakthrough curve · Column · Encapsulation · Isotherms · Kinetics

Introduction

Many dyestuffs were used in textile dyeing and printing processes, which are non-biodegradable. Among the dyes, anionic dyes are carcinogenic and have the highest risk of diseases due to its toxic in nature. The presence of ethylene glycol in AB-FFS dye is responsible for producing a variety of illnesses such as proteinuria, uremia and anuria which are toxic to the liver and kidney [1, 2]. In recent days, treating the anionic dyes becomes a big challenge and several methods failed to produce satisfactory results.

Based on previous reports, adsorption methods do offer the most efficient technique used for the removal of dyes and pigments from industrial effluents. Adsorbents such as activated carbon [3], pith carbon [4], bagasse fly ash [5], rice husk [6] and cashew nut shell [7] have been used for dye decolorization under the batch mode. All these adsorbents had limited success over the industrial effluent treatments. Moreover, equilibrium data from batch mode provides fundamental information, but not applicable for real-time process. Therefore, there is a need to investigate the fixed bed column study to obtain engineering data for scaling up from laboratory-scale to pilot-scale level. Recently, a variety of natural adsorbents such as pistachio hull waste [8], dried *Moringa oleifera* seeds [9], orange peel cellulose [10] and *Artocarpus heterophyllus* [11] have been reported for the removal of heavy metals and dyes.

Earlier studies have confirmed that *Moringa oleifera* seed as biosorbent, which has polypeptides of molecular weight ranging from 6 to 16 kDa and its isoelectric pH value 10, contains high zeta potential, and cationic and anionic properties. Considering these properties, *Moringa oleifera* could be used as a good biosorbent when it is encapsulated. Our previous studies have reported that encapsulated *Moringa oleifera* beads are effectively used for the removal of

✉ Wilson Richard Thilagaraj
thilagaraj.richard@gmail.com

¹ Department of Biotechnology, School of Bioengineering, SRM University, Kattankulathur 603203, Tamil Nadu, India

² Department of Chemical Engineering, School of Bioengineering, SRM University, Kattankulathur 603203, Tamil Nadu, India

heavy metals [9]. Hence, this present study is focused on the performance of encapsulated *Moringa oleifera* seed powder by cross-linking with polymer Ca-alginate, to obtain stable beads and used for its biosorption efficiency for AB-FFS solution. The biosorbent was investigated in batch as well as fixed bed column packed with MEA with respect to flow rate and bed height. Eventually, the isotherm, kinetics and breakthrough curve analysis for the removal of AB-FFS dyes were investigated.

Materials and methods

Preparation of dye solutions

The Anionic Blue-FFS dye was manufactured by Dynamic Industries Ltd, India. It is an anionic dye which is referred to as Anionic Blue-15 with a chemical formula: $C_{42}H_{46}N_3NaO_6S_2$ and molecular weight: 775.95. This product is commercially available as CI No: 42665. The chemical structure of the Anionic Blue-FFS dye has attributed to Lecotan Blue-AC, Triacid Blue-B, Raviramine Blue-BS and Dinacid Brilliant Blue-B, which is shown in Fig. 1. Synthetic AB-FFS dye solutions were prepared by adding the desired amount of dye in double-distilled water to obtain a stock solution of 1000 mg/L. The working solution was diluted to the required concentration of the experiments.

Preparation of biosorbent

Dried *Moringa oleifera* seeds were de-shelled and fresh white kernels were washed several times with de-ionized water and air dried. Then, kernels were pulverized and converted into a fine powder with an approximate size range from 300 to 500 μm . MEA were prepared using 2 % of alginate solution was mixed with kernel powder in the ratio of 1:5 to form a suspension solution which was converted

into Ca-alginate beads by a phase inversion technique using 3 % of calcium chloride solution with the help of the peristaltic pump. The flow rate of the pump was adjusted to 250 spherical beads per hour. After encapsulation, MEA in the calcium chloride solution was incubated at room temperature for 2 h for stability, which led to the complete replacement of sodium ions by calcium ions. Eventually, the beads were dried and washed with 99 % of ethanol for complete sterilization for storage long periods [9]. In addition, the physical appearances and properties of the MEA have been characterized such as BET surface area, porosity, bulk density and stability as shown in Table 1.

Instrumental analysis

The surface morphology of MEA was identified by scanning electron microscopy (SEM) using an Agilent Technology scanning probe microscope. The surface functional groups of MEA were determined by Fourier transform infrared reflection (FTIR) measurements using an ALPHA FT-IR spectrometer. The zeta potential curve of the MEA was analyzed using a (Zetasizer 2000) Malvern Zeta meter.

Batch biosorption studies

Batch biosorption experiments were carried out in 250 ml Erlenmeyer flasks containing 100 ml of AB-FFS initial dye concentrations (25, 50, 75 and 100 mg/L) with the desired amount of MEA (1 g/100 mL). The effect of pH was investigated on the dye in the range of 2–10 pH and the effect of temperature was investigated in the range of 323–343 K. The pH of the solution was adjusted using 0.1 M of HCl and 0.1 M of NaOH solutions. The flasks were agitated in the orbital shaker (Orbitek, Scigenics Biotech) at 100 rpm. Samples were collected at regular intervals. The residual concentration of dyes in the supernatant of each sample was measured using UV–VIS spectrometer at 560 nm using JASCO, UV–670. One set of experiment was conducted using Ca-alginate beads, which is free from *M.oleifera*. The equilibrium dye adsorbate q_e (mg/g) was calculated using the following formula (1):

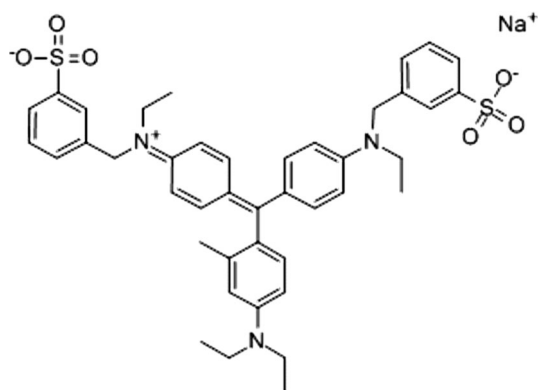


Fig. 1 Structure of anionic blue-FFS dye

Table 1 The physical appearance and properties of MEA beads

Parameters	Values
Porosity (%)	40–45
Bulk density (g/cm^3)	1.5
Stability	Stable and rigid
Mean diameter (mm)	1.75–2.25
BET surface area (m^2/g)	14.5
q_{max} (mg/g)	0.0167
Pore volume (cm^3/g)	0.05

$$q_e = (C_o - C_e/m)V, \quad (1)$$

where C_o and C_e are the initial and final dye concentration in mg/L; V is the volume of the dye solution (L); m is the dry weight of the biosorbent (g).

Fixed bed column studies (FBC)

The fixed bed column reactor was made up of Perspex tubes of 4.5 cm internal diameter and 55 cm in height and the beads (MEA) packed with different heights such as 5, 10 and 15 cm. In this experiment, a known concentration of AB-FFS dye was pumped at different flow rates to a known height of the adsorbent. The particle size of the adsorbent used in the experiment was 2.0 ± 0.1 mm. The samples were collected from the column at regular intervals and the absorbance of the color was measured using a UV–VIS spectrometer at 560 nm. The continuous process flow diagram is shown in Fig. 2.

Computational statistics and mathematical modeling

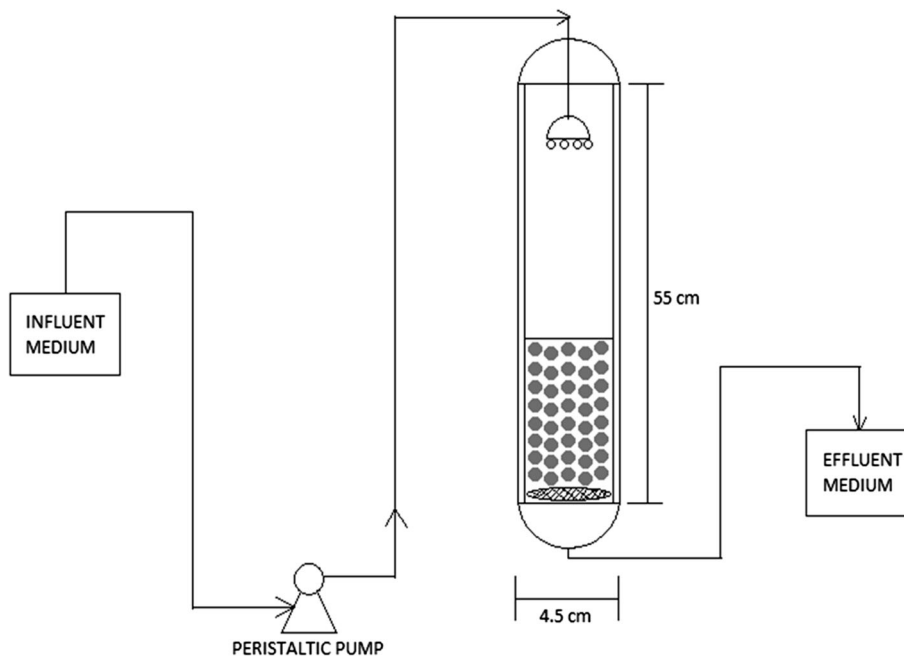
Batch experiments were analyzed in triplicate ($N = 3$) and the data reveals the mean values which represent the error bars. Regression, the correlation coefficient, standard deviation was calculated using SSPC PC + TM statistical package, 1983. Multiple mean comparisons using least significant difference were computed using the significance level ($p < 0.05$). To investigate the data, two inherent

models like Langmuir and Freundlich were used to describe the mechanism of biosorption and to find the maximum biosorption capacity of the adsorbents at different temperatures. The results from the effect of temperature were used to calculate the thermodynamic parameters such as free energy, enthalpy and entropy. Eventually, to access the kinetic parameters, the data with different concentrations results were analyzed using pseudo-first-order, pseudo-second-order and intraparticle diffusion models. To consider, the best fit model to describe the performance of the breakthrough curves, regression coefficients (R^2) can be fit between experimental and theoretical values of Thomas and Yoon–Nelson equations.

Desorption studies

For batch desorption experiments, deionized water and 0.1 M of analytical-grade NH_4Cl , EDTA, CH_3COOH , HCl, HNO_3 and NaOH were used. In this study, a series of 250 ml of Erlenmeyer flasks containing 100 mL of desorption solution was mixed with 10 g of dye-loaded MEA at room temperature. The mixed solution was agitated in an orbital shaker (Orbitek, Scigenics biotech) at 200 rpm for 1 h. The MEA was removed from the solution and centrifuged at 1000 rpm for 5 min and the desorbed concentrations were analyzed using a UV-spectrometer. After each cycling experiments, beads were washed with distilled water thrice and then treated again in 100 mg/L concentration of AB-FFS dye.

Fig. 2 Continuous process flow diagram



Results and discussion

Characterization of biosorbent

The morphology of MEA was investigated before and after biosorption using SEM analysis. From Fig. 3a, the micrograph of dried MEA reveals, the presence of the porous matrix structure which has a rough and a heterogeneous surface area for biosorption. The same bead was examined after biosorption as shown in Fig. 3b. Almost all the porous matrix structures completely disappeared and it clearly depicts that the functional groups present in the MEA provide active sites for AB-FFS to bind and there is much difference in the adsorbent structure (i.e., absence of the porous matrix). The FTIR spectra of MEA before and after biosorption were analyzed as shown in Fig. 3c. A characteristic band at 2902 and 2862 cm^{-1} is attributed to C–H of CH_2 groups of proteins and at 1800–1600 cm^{-1} is attributed to the C=O bond stretching that defines the presence of a carbonyl group of the fatty acid [12]. The peak that appears at 1627 cm^{-1} may be attributed to the N–H (amine) groups present in the protein portions of the MEA. On the other hand, an FTIR spectrum of MEA after biosorption shows the disappearance of the two peaks, which is due to the mechanism of cross-linking of MEA which could be either by de-protonation or ionic interaction [9]. In addition, the point of zero charge (pH_{zpc}) was examined for MEA beads, and the results showed that the pH_{zpc} is 4.9–5.1 as shown in Fig. 3d. It can be used to explain the influence of pH on biosorption. When the pH value is lower than pH_{zpc} , the surface charge of the MEA is positive and hence the biosorption capacity decreases. Similarly, the value of pH is greater than pH_{zpc} , and the surface charge of the MEA has a higher negative charge, which results in higher attraction of the dyes.

Batch biosorption studies

Effect of initial pH and pH_{zpc}

The pH varies the surface charge properties of the reactant so that the adsorbate or adsorbent can bind to the active site to undergo reactions. The effect of pH on the biosorption capacity of the AB-FFS dye with concentration of 100 mg/L was studied in the range of 2–10. The influence of pH on the biosorption can be explained on the basis of point of zero charge (pH_{zpc}), which is the point at which the net charge of the biosorbent is zero. From Fig. 4a, it can be seen that the degree of AB-FFS biosorption onto MEA decreased from 95.01 to 17.53 % when the pH was increased from 2 to 10. It can be explained by the pH_{zpc} of the adsorbent and the nature of the AB-FFS dye (anionic). The pH_{zpc} of the MEA

is around 4.9–5.1, which explains that the surface of the adsorbent is positively charged at under pH 5.1 [9]. At lower pH, large amount of H^+ ions is present on the surface of the biosorbents, which favors strong electrostatic attraction and hence maximum rate of biosorption. As the increasing pH (>5) value, the biosorption decreased gradually due to the OH^- ions forms the negative charge on the surface of the adsorbents which do not bind to the anionic adsorbate, thus reduces the rate of biosorption due to the electrostatic repulsion [13]. Thus, a maximum AB-FFS biosorption was attained at an optimum pH of 2. Further, the rest of the experiments were conducted at pH 2.

Effect of initial dye concentration

The study of initial dye concentration influences the performance of MEA and provides information about driving force to overcome all mass transfer resistance between the solid and aqueous phase. The biosorption of AB-FFS concentration was investigated at 25–100 mg/L up to 500 min for all the concentrations using 1.0 g of MEA at room temperature under pH 2. From Fig. 4b, the equilibrium biosorption was observed at 300 min and was found to be a maximum of 98.5 ± 0.5 % for 25 mg/L and minimum of 90.85 ± 1.25 % for 100 mg/L, respectively. At lower AB-FFS concentrations, the dye molecules present in the aqueous solution interacted with the active sites available on the solid surface, facilitating higher biosorption. Consequently, the increase of initial AB-FFS concentration resulted in a reduction of its biosorption percentage due to the limited number of binding sites and more dye molecules were left unabsorbed in the solution resulting in lower rate of biosorption [8, 14].

Effect of temperature and thermodynamic studies

The effect of temperature is an important biosorption parameter to investigate the stability of MEA. From Fig. 4c, it was found that biosorption rate was increased with the increase in temperature. As the temperature increased from 323 to 343 K, it was observed that biosorption porosity increased with a decrease in viscosity of the solution and thereby increased the diffusion rate [8]. Endothermic chemical interaction and disaggregation lead to an increase in temperature. From this experiment, it was found that MEA biosorption was quite good and stable even at higher temperature [15, 16]. Thermodynamic parameters such as Gibbs free energy change (ΔG°), standard enthalpy change (ΔH°) and standard entropy change (ΔS°) are calculated to understand more about the effect of temperature on the biosorption. Biosorption experiments were calculated at different temperatures (323, 333 and 343 K) using the following equations:

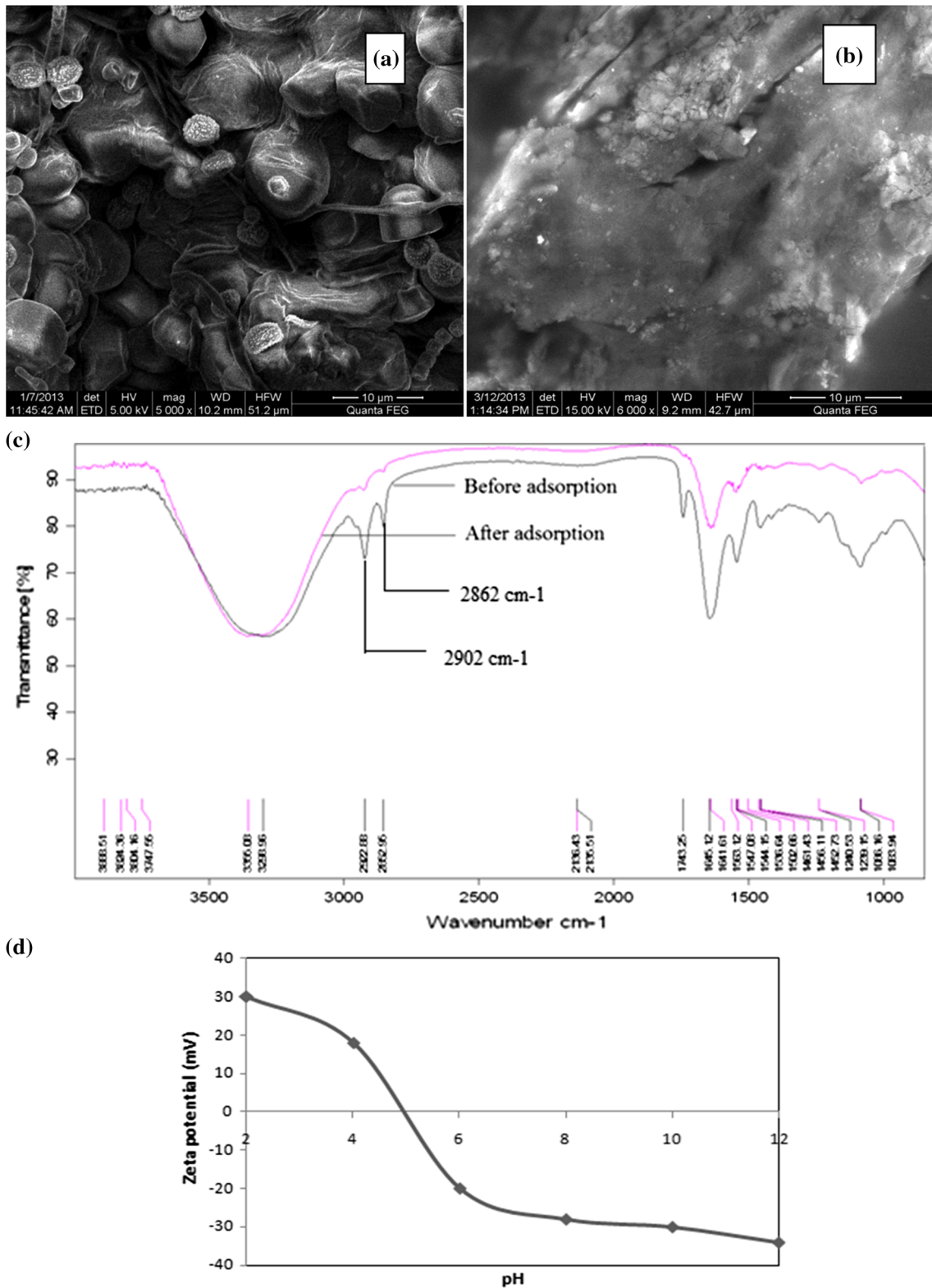


Fig. 3 SEM images before biosorption (a) and after biosorption (b). c FTIR spectra before and after biosorption. d Zeta potential–pH profile

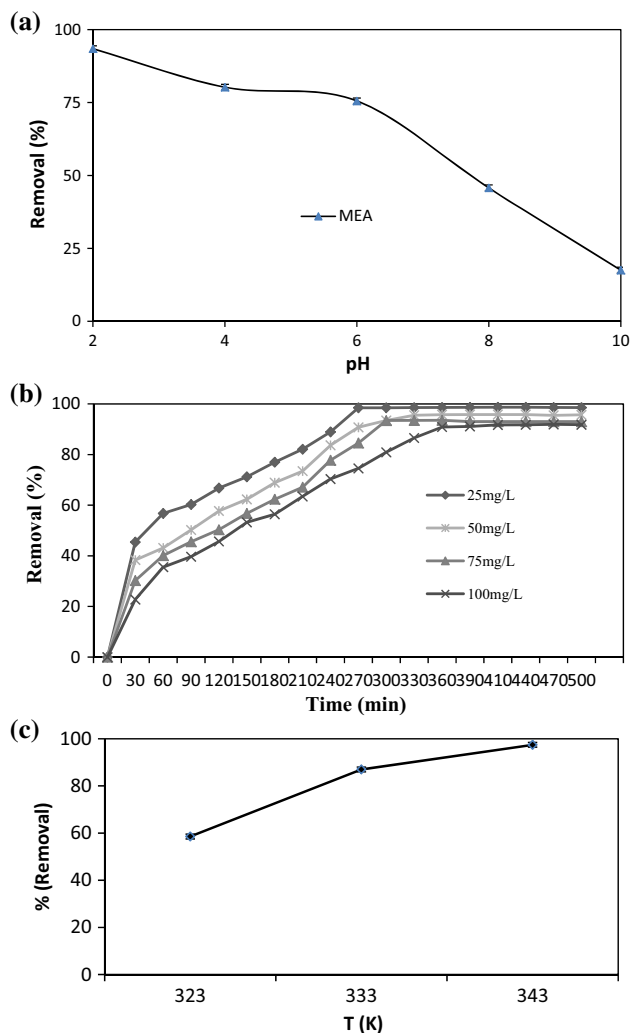


Fig. 4 Batch biosorption of AB-FFS onto MEA: **a** influence of pH (2–10), **b** influence of initial dye concentrations (25–100 mg/L) and **c** influence of temperature (323, 333 and 343 K). Experimental conditions: synthetic AB-FFS solution volume: 100 mL; contact time: 8 h; biosorbent mass: 1 g; agitation speed: 100 rpm; Error bars represent SD

$$K_c = C_a/C_e, \quad (2)$$

$$\Delta G^\circ = -RT \ln K_c, \quad (3)$$

$$\Delta G^\circ = \Delta H^\circ - T\Delta S^\circ, \quad (4)$$

where K_c is the distribution coefficient for the adsorption; C_a is the amount of dye (mg) adsorbed on the adsorbent per liter of the solution at equilibrium and C_e is the equilibrium concentration (mg/L) of the dye in the solution. R is the universal gas constant (8.314 J/mol K) and T (°K) the absolute temperature. The standard enthalpy (ΔH°) and entropy (ΔS°) of adsorption were determined from the Vant Hoff Eq. (5):

$$\ln K_c = [(\Delta S^\circ)/R - \Delta H^\circ/RT]. \quad (5)$$

ΔH° and ΔS° were obtained from the slope and intercept of the Vant Hoff plot of $\ln K_c$ versus $1/T$. The values of ΔG° , ΔH° and ΔS° under different temperature are listed in Table 2. The negative values of ΔG° reveal that the biosorbent was spontaneous. The values of Gibbs free energy decreases with an increase in temperature which signifies that MEA is favorable for biosorption. The positive value of ΔH° and ΔS° indicates that the biosorption is an endothermic reaction and there is randomness at the solid–solution interface [17].

Biosorption isotherm modeling

To perform the characterization of the biosorption behavior of the dye, the equilibrium adsorption isotherms on MEA at pH 2 with different temperatures were obtained for the AB-FFS dye. Therefore, these equilibrium data are an essential source for practical design and fundamental understanding behavior of the carrier matrix for MEA. There are few nonlinear regression equations well described by various models. In this study, Langmuir [18] and Freundlich [19] model was chosen and it provides a scrupulously accurate method to reveal the linearity fitting and to explain how the AB-FFS dye interacts with MEA. The equations are listed as follows:

The general form of the Langmuir model is given by

$$C_e/q_e = 1/q_{\max}K_L + C_e/q_{\max}, \quad (6)$$

where q_{\max} (mg/g) is the maximum biosorption capacity at equilibrium; K_L (L/mg) is the Langmuir binding constant; q_e gives the value of the sorbed capacity at equilibrium time (mg/g); C_e is the equilibrium concentration of the adsorbed ions (mg/L). The values of q_{\max} and K_L were estimated from the slope and intercept of the linear plots of C_e/q_e against C_e using values from the batch experiments.

The general form of the Freundlich model is given as

$$\ln q_e = \ln K_{Fr} + 1/n \ln C_e, \quad (7)$$

where the K_{Fr} ($\text{mg}^{1-1/n} \text{L}^{1/n} \text{g}^{-1}$) value gives the relative biosorption capacity of the adsorbent and $1/n$ is the dimensionless Freundlich adsorption intensity value. The values of K_{Fr} and n can be determined by plotting $\ln q_e$ versus $\ln C_e$ resulting in a straight line with a slope of n and an intercept of $\ln K_{Fr}$. A higher value of K_{Fr} estimates provide higher affinity toward the ions and the value of $1/n$ lies between $0.1 < 1/n < 1$ representing favorable biosorption [20].

The detailed parameters of Langmuir and Freundlich isotherm equations are listed in Table 3. From the Langmuir isotherm, the maximum monolayer adsorption capacity of MEA increased from 18.18 to 76.92 (mg/g) with the increase of the solution temperature from 323 to

Table 2 Thermodynamic parameters of AB-FFS onto MEA at different temperatures

Dye concentration (mg/L)	ΔG° (kJ/mol)			ΔH° (kJ/mol)	ΔS° (J/mol K)
	323 K	333 K	343 K		
25	−4331	−8416	−11,093	89.14	284
50	−1889	−7378	−9268		
75	−7277	−6285	−9096		
100	−3007	−5924	−8697		

Table 3 Isotherm parameters for the biosorption of AB-FFS dye onto MEA

MEA (K)	Langmuir				Freundlich			
	q_m (mg/g)	K_L (L/mg)	R^2	R_L	K_{Fr} mg ^(1−n) L ^{1/n} /g	n	R^2	
323	18.18	0.028	0.935	0.41	0.431	1.315	0.998	
333	23.8	0.039	0.957	0.46	2.488	0.654	0.998	
334	76.92	0.091	0.995	0.52	2.557	0.781	0.989	

343 K, respectively, which confirms that the process is an endothermic reaction. The correlation coefficients (R^2) are listed in Table 3, strongly indicating that the biosorption of AB-FFS onto MEA follows both the Langmuir and Freundlich isotherm model.

MEA biosorption was further analyzed in terms of separation factor; R_L is a dimensional parameter which is defined as $R_L = (1/1 + K_L C_0)$, derived from the Langmuir equation and C_i is the initial dye concentration. R_L indicates the biosorption process to be either favorable ($0 < R_L < 1$), unfavorable ($R_L > 1$), linear ($R_L = 1$) or irreversible ($R_L = 0$). From Table 3, R_L values gradually increase from 0 to 1, which indicates the process is more favorable, and higher temperature may enhance biosorption process.

Biosorption kinetics modeling

To examine the controlling mechanism of biosorption as well as to understand the behavior of the AB-FFS dye onto the beads, the three kinetics model was investigated: pseudo-first order kinetics, pseudo-second order kinetics followed by Weber and Morris intraparticle diffusion model. In this study, the kinetics of biosorption of two different concentrations of AB-FFS dye (50 and 100 mg/L) onto MEA was carried out with the pseudo-first-order kinetics by Lagergren's [21] and pseudo-second-order model by Ho and McKay's [22] followed by Weber and Morris's intraparticle diffusion model [23].

For the biosorption of AB-FFS, the first-order kinetics can be represented by Eq. 8:

$$\log(q_e - q_t) = \log q_t - K_1 t / 2.303, \quad (8)$$

where q_e and q_t are the amounts of AB-FFS dye adsorbed (mg/g) at equilibrium and at time t (h), respectively, and K_1 is the adsorption rate constant (min^{-1}). The Lagergren

first-order kinetic constant (K_1) and the theoretical value of (q_e) can be obtained from the linear plots of $\log(q_e - q_t)$ against time for 50 and 100 mg/L of initial dye concentrations as shown in Fig. 5a. From the Fig. 5a, the plot was found to be linear and the correlation coefficient (R^2) was greater than 0.9, which indicates that pseudo-first order were appropriate for the use of AB-FFS dye onto MEA. The rate constant (K_1) and q_e (exp) values along with the correlation coefficient (R^2) are listed in Table 4. The data was further validated using second-order kinetics, which can be expressed by Eq. 9:

$$t/q_t = 1/K_2 q_e^2 + t/q_e. \quad (9)$$

For the pseudo-second-order kinetic model, the plots of t/q_t against time at 50 and 100 mg/L initial dye concentrations are shown in Fig. 5b. The value of q_e (mg/g) and second-order kinetic constants k^2 (g/mg min) along with correlation coefficients of MEA are listed in Table 4. In addition from Table 4, it was noticed that the theoretical predicted q values were not concordant with the experimental values and R^2 values were not in accordance, suggesting that the use of MEA on AB-FFS dye did not fit well with the second-order kinetics. Further, Weber and Morris found a kinetic process of liquid–solid adsorption of intraparticle diffusion and mass action. To identify the diffusion mechanism, the relationship between q_t and $t^{1/2}$ could be written in the form of Eq. (10) given by:

$$q_t = K_p t^{1/2} + C, \quad (10)$$

where q_t (mg/g) is the amount of dye adsorbed at various times (t), K_p is the intraparticle diffusion rate constant (mg/g $\text{min}^{0.5}$) and C is the intercept of the line which is directly proportional to the boundary layer of thickness. This multi-linear Eq. 10 involves three steps. The first step is the



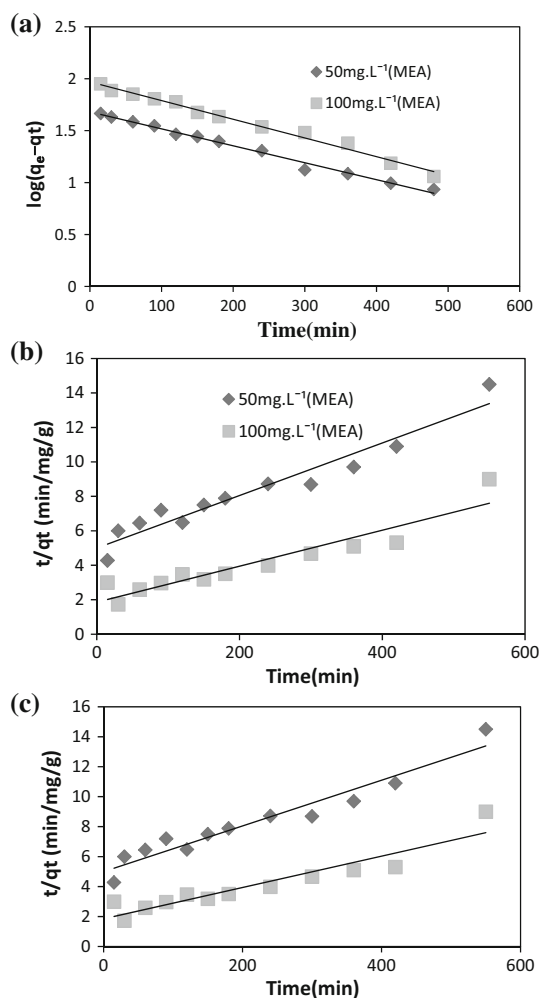


Fig. 5 Pseudo-first-order model (a), Pseudo-second-order model (b) and intraparticle diffusion model (c) for batch adsorption of AB-FFS dye onto MEA. Experimental parameters—dosage 1 g, volume 100 ml, dye concentration 50 and 100 mg/L, temperature 273 K, pH 2, reaction time 500 min

immediate process that allows quick adsorption, the second step is the intraparticle diffusion stage, whereas the final stage is the equilibrium step in which the solute moves slowly from macropores to micropores causing a slow adsorption rate [8, 22]. A plot of q_t against $t^{1/2}$ should be linear, from which K_p and C can be calculated from the slope and intercept of the plot. According to Weber and Morris, if the intraparticle diffusion is the rate-limiting

step, it is necessarily the plot of q versus $t^{1/2}$ which passes through the origin.

The intraparticle diffusion of AB-FFS onto MEA at an initial dye concentration of 50 and 100 mg/L is illustrated in Fig. 5c. It was observed that the straight line of the intraparticle region of MEA of 100 mg/L did not pass through the origin, while the rest pass through the origin. Moreover, it is clear from Table 4 that MEA diffusion of 100 mg/L has a larger intercept C value, which relates high boundary layer resistance and the surface adsorption in the rate-limiting step. According to McKay, the boundary layer thickness retards the intraparticle diffusion. Table 4 clearly explains that the intraparticle parameter K_p values increase along with increasing dye concentrations. Thus, the increase of AB-FFS concentrations results in an increase in the diffusion rate of dye into pores of the beads. Especially, MEA increases regularly for 50 mg/L (5.09 mg/g min^{0.5}) and 100 mg/L (9.25 mg/g min^{0.5}) with low K_p value.

Fixed bed column study

The performance of the MEA biosorbent was tested in a fixed bed column, to check the feasibility of the MEA in real-time effluents. The AB-FFS solution (100 mg/L) was fed through the column of different bed heights (5 and 15 cm) with two different flow rates (1, 2 and 5 mL/min) and the samples were collected at regular intervals.

Effect of bed height

The effect of bed height is an important parameter for calculating the design of the FBC performance. At a constant initial AB-FFS concentration (100 mg/L) and flow rate (2 mL/min), the breakthrough curve for biosorption of the AB-FFS onto MEA of two different bed heights (BH) such as 5 cm (12.25 g) and 15 cm (36.75 g), respectively, is shown in Fig. 6. From Fig. 6a, both the breakthrough times, t_b and exhaustion time t_e , were found to increase with increasing bed height, whereas the shape of the breakthrough was slightly different with the variation of bed height. From Fig. 6a, an earlier breakthrough and exhaustion time was attained in BH—5 cm ($t_b = 33$ th min and $t_e = 340$ th min) and BH—15 cm ($t_b = 150$ th min and $t_e = 420$ th min), respectively. An increase in dye uptake

Table 4 Kinetic parameters for the biosorption of AB-FFS dye onto MEA

MEA	Pseudo-first-order kinetics				Pseudo-second-order kinetics			Intraparticle diffusion		
	q_e (exp) (mg/g)	q_e (cal) (mg/g)	k_1 (min ⁻¹)	R^2	q_e (cal) (mg/g)	k_2 (g/mg min)	R^2	k_p (mg/g min ^{0.5})	C	R^2
50 mg/L	47.8	47.863	0.1428	0.990	66.66	0.2001	0.932	5.09	2.93	0.993
100 mg/L	94.55	93.118	0.1756	0.987	100	0.5391	0.876	9.25	7.74	0.982



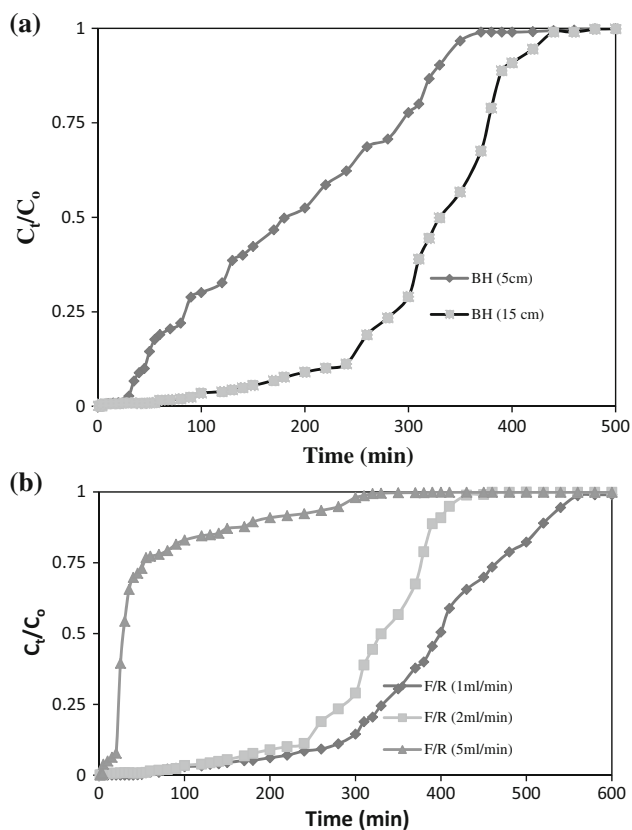


Fig. 6 **a** Breakthrough curves for biosorption of AB-FFS onto MEA at different bed heights (BH-5 and 15 cm with constant flow rate 2 mL min^{-1} and initial concentration 100 mg/L). **b**. Breakthrough curves for biosorption of AB-FFS onto MEA at different flow rates (1, 2 and 5 mL/min with constant BH-15 cm and initial concentration 100 mg/L)

was observed at elevated bed height due to the increase in the amount of the MEA. As the bed height increases, simultaneously, the mass transfer zone (MTZ) also increases in the column, which moves downward from the entrance of the bed to the exit.

Effect of flow rate

The effect of varying flow rate is an important parameter which determines the contact time of the dye with the biosorbent in the FBC. The breakthrough curves C_t/C_o against time (min) for three different flow rates (1, 2 and 5 mL/min) with constant bed height of 15 cm were investigated and shown in Fig. 6b. From the figure, as the flow rate increases, the breakthrough curve becomes steeper and the biosorbent achieves early saturation at 5 mL/min . Similarly, at lower flow rate, a longer contact time with the shallow biosorption zone results in a higher uptake of AB-FFS. From Fig. 6b, earlier breakthrough and exhaustion time were attained flow rates (F/R) 1 mL/min ($t_b = 170 \text{th min}$ and $t_e = 540 \text{th min}$), 2 mL/min

($t_b = 140 \text{th min}$ and $t_e = 410 \text{th min}$) and 5 mL/min ($t_b = 10 \text{th min}$ and $t_e = 280 \text{th min}$), respectively.

Modeling of breakthrough curves

Fixed bed column data obtained were further analyzed for their breakthrough behaviors using two different mathematical equation models such as those of Thomas [24] and Yoon–Nelson [25]. The biosorption performance was assessed at an initial concentration ratio, $C_t/C_o > 0.05$, consequently, 5 % breakthrough until $C_t/C_o > 0.95$ that is, 90 % breakthrough for dye decolorization by considering water quality and operating limits of MTZ of the column [26].

Applications of the Thomas model

The experimental data were fitted to the Thomas model to determine the maximum dye biosorption capacity of the column (q_o) and the Thomas rate constant (k_{Th}), as shown in Table 5. Further, this model is based on the assumption that the process follows Langmuir isotherms of equilibrium with no axial dispersion and the rate driving force which obeys the second-order reversible reaction kinetics [27]. The linearized form of Thomas model Eq. (11) can be expressed as follows:

$$\ln\left(\frac{C_o}{C_t} - 1\right) = \frac{k_{Th} q_o m}{v} - \frac{k_{Th} C_o}{vt}, \quad (11)$$

where k_{Th} (mL/mg/min) is the Thomas rate constant, q_o (mg/g) is the equilibrium adsorbate uptake per gram of the biosorbent, C_o and C_t (mg/L) are the inlet and outlet concentrations (g), m is the mass of the adsorbent in the column, and v (mL/min) stands for flow rate. The value C_t/C_o is the ratio of the outlet to inlet effluent concentrations. By plotting the linear plots of $\ln[(C_o/C_t) - 1]$ against time (t), the rate constant value (k_{Th}) was determined and the maximum capacity of biosorption (q_o) was obtained from the slope and intercepts using values from the column experiments. The regression coefficient (R^2) and the relative constants such as q_o (mg/g) and k_{Th} values were calculated from the experimental data as shown in Table 5. The regression coefficients (R^2) were between 0.8 and 0.9, which showed that the experimental data fitted the Thomas model well. From Table 5, in general, it was observed that by increasing the flow rate, the biosorption capacity (q_o) decreased, but the values of the rate constant (k_{Th}) increased. Further, by extending the bed height, the values of q_o decreased and the k_{Th} value increased significantly. In addition, from Table 5, it was found that 15 cm of bed height (BH) with 1 mL/min F/R gives maximum biosorption values (q_o , 1543 mg/g).



Table 5 Thomas and Yoon–Nelson model parameters for the removal of AB-FFS using MEA at different conditions using linear regression analysis

Bed height (cm)	Flow rate (mL/min)	Thomson model					Yoon–Nelson model				
		K_{TH} (mL/min mg)	q_{exp} (mg/g)	q_{the} (mg/g)	ε %	R^2	K_{YN} (/min)	τ_{exp} (min)	τ_{the} (min)	ε %	R^2
5	2	0.00046	447	458	2.35	0.867	0.022	180.01	182.09	2.35	0.867
15	1	0.00015	1505	1543	4.01	0.785	0.015	203.1	205.7	4.01	0.785
15	2	0.00047	801	806	5.35	0.902	0.023	190	191.9	5.35	0.903
15	5	0.001	367	380	5.01	0.805	0.019	94.5	96	5.01	0.806

Application of the Yoon–Nelson model

A theoretical model developed by Yoon–Nelson was useful to investigate the breakthrough behavior of AB-FFS on MEA. In addition, this model was derived based on the assumption that the rate of decrease in the probability of biosorption for each adsorbate molecule is proportional to the probability of adsorbate biosorption and the probability of an adsorbate breakthrough on the biosorbent [25, 28]. The linearized model of a single component system is expressed as in Eq. 12:

$$\ln\left(\frac{C_t}{C_0 - C_t}\right) = k_{YN} t - \tau k_{YN}, \quad (12)$$

where, k_{YN} (1/min) is the Yoon–Nelson rate constant and τ (min) is the time required for 50 % adsorbate breakthrough. The values of k_{YN} and τ were estimated from the slope and intercepts of the linear graph between $\ln[(C_t)/(C_0 - C_t)]$ versus time t at different flow rates with different bed heights and the values of k_{YN} and τ are illustrated in Table 5. From Table 5, the values of k_{YN} were found to increase with higher F/R and lower BH; however, it decreased with lower F/R and higher BH. Nevertheless, τ (the time required for 50 % breakthrough) was higher at lower F/R and higher BH. In addition, from Table 3, it was found that the τ (min) values of 205 min and 223 min were obtained at 15 BH with F/R 1 mL/min and 15 BH with F/R 2 mL/min. The values of the regression coefficient (R^2) are listed in Table 5 and it was found that almost all the values of R^2 were between the range of 0.8 and 0.9. Furthermore, there is good concurrence between the predicted and experimental data which provide the best fit to the Yoon–Nelson model.

Desorption studies

To improve the cost-effectiveness in industries, reusability of the biosorbent is an important factor in practical applications for dye removal from wastewaters. The reusability of MEA beads can be determined by its biosorption

performance in consecutive biosorption/resorption cycles under batch mode and the desorption efficiencies are compared in Fig. 7. From the figure, the use of deionized water was found to be negligible (<5 %). Further, the use of NH_4Cl was resorbed by only <20 %, whereas CH_3COOH and EDTA give 50–60 % of the desorption efficiency. The use of acids such as HNO_3 and HCl gives more than 90 % de-resorption efficiency which can be attributed to the fact that the AB-FFS dyes react faster with acids than bases. On the other hand, during the desorption process, $NaOH$ reacts with calcium-alginate beads and it was completely dissolved due the replacement of calcium and sodium ions. Overall, HNO_3 and HCl was found to have higher resorption efficiencies and similar work has been reported previously [29, 30]. The overall MEA adsorbent was found to be cost-effective and feasible for treatment of industrial wastewater treatment.

Conclusion

This research work introduced the encapsulated *Moringa oleifera* beads as a potential biosorbent for dye removal in the batch as well as in continuous column studies which gave more than 90 % of removal efficiency. The maximum

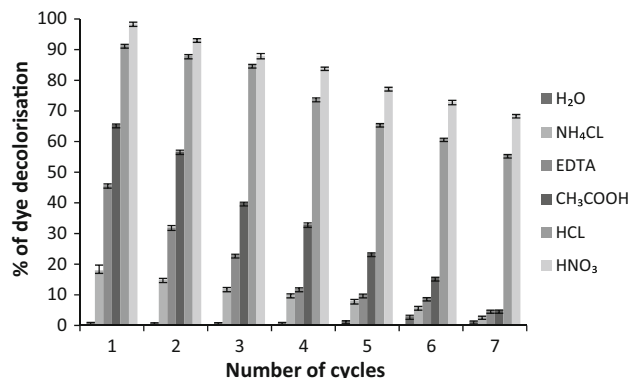


Fig. 7 Desorption efficiency of AB-FFS dye onto MEA using different desorbing agents (concentration: 0.1 M)

biosorption capacity of AB-FFS dye calculated from Langmuir isotherm, which can be well fitted onto MEA of 18.18, 23.80 and 76.92 mg/g, respectively, was studied from 323 to 343 K. The thermodynamic parameter results reveal that the biosorbent was spontaneous and it was an endothermic reaction process. Among the kinetic model studies, the biosorption kinetics favor both pseudo-first-order and intraparticle diffusion model. In fixed bed column studies, data obtained were fitted with well-established models, namely Thomas and Yoon–Nelson. Overall, this research showed that MEA is a potential and promising alternative biosorbent for removal of color from textile effluents. Moreover, dried *Moringa oleifera* is a biological waste material that is easily viable and biodegradable.

Open Access This article is distributed under the terms of the Creative Commons Attribution 4.0 International License (<http://creativecommons.org/licenses/by/4.0/>), which permits unrestricted use, distribution, and reproduction in any medium, provided you give appropriate credit to the original author(s) and the source, provide a link to the Creative Commons license, and indicate if changes were made.

References

- Lin SH, Lou CC (1996) Treatment of textile wastewater by foam flotation. *Environ Technol* 17:841–849
- Kaneko S (1982) Adsorption of several dyes from aqueous solutions on silica-containing-oxide gels. *Sep Sci Technol* 17:1499–1510
- Juang RS, Swei SL (1996) Effect of dye nature on its adsorption from aqueous solutions onto activated carbon. *Sep Sci Technol* 31:2143–2156
- Namasivayam C, Kavitha D (2003) Adsorptive removal of 2-chlorophenol by low-cost pith carbon. *J Hazard Mater* 98:257–270
- Gupta VK, Jain D, Mohan S, Sharma M (2000) Removal of basic dyes (Rhodamine-B and Methylene blue) from aqueous solutions using bagasse fly ash. *Sep Sci Technol* 35:2097–2113
- Saha P (2010) Study on the removal of methylene blue dye using chemically treated rice husk. *Asian J Water Environ Poll* 7:2
- Ponnusamy SK, Subramaniam R (2013) Process optimization studies of Congo red dye adsorption onto cashew nut shell using response surface methodology. *Int J Ind Chem* 4:17
- Moussavi G, Khosravi R (2011) The removal of cationic dyes from aqueous solutions by adsorption onto pistachio hull waste. *Chem Eng J Res Des* 89:2182–2189
- Radhakrishnan K, Lakshmi S, Radha P, Aparna N, Vishali S, Thilagaraj WR (2016) Biosorption of heavy metals from actual electroplating wastewater using encapsulated *Moringa oleifera* beads in fixed bed column. *Desalin Water Treat* 57:3572–3587
- Lai Y, Thirumavalavan M, Lee J (2010) Effective adsorption of heavy metals ions (Cu^{2+} , Pb^{2+} , Zn^{2+}) from aqueous solution by immobilization of adsorbents on Ca-alginate beads. *Toxicol Environ Chem* 92:697–705
- Radhakrishnan K, Aparna N, Thilagaraj WR (2015) Effective and ecofriendly nano biosorbent for treatment of textile wastewater. *Res J Chem Environ* 19:14–23
- Araujo CST, Melo EI, Alves VN, Coelho NMM (2010) *Moringa oleifera* Lam. seeds as a natural solid adsorbent for removal of Ag in Aqueous solutions. *J Brazilian chem soc* 21:1727–1732
- Nassar NN (2010) Kinetics, mechanistic, equilibrium, and thermodynamic studies on the adsorption of acid red dye from waste water by $\gamma\text{Fe}_3\text{O}_4$ nanoadsorbents. *Sep Sci Technol* 48:1092–1110
- Xi Y, Shen Y, Yang F, Yang G, Liu C, Zhang Z, Zhu D (2013) Removal of azo dye from aqueous solution by a new biosorbent prepared with *Aspergillus nidulans* cultured in tobacco wastewater. *J Taiwan Ins Chem Eng* 44:815–820
- Bouhamed F, Elouear Z, Bouzid J (2012) Adsorption removal of copper (II) from aqueous solutions on activated carbon prepared from Tunisian date stones: equilibrium, kinetics and thermodynamics. *J Taiwan Inst Chem Eng* 43:741–749
- Qiu B, Cheng X, Sun D (2012) Characteristics of cationic Red X-GRL biosorption by anaerobic activated sludge. *Bioresour Technol* 113:102–105
- Inbaraj BS, Sulochana N (2006) Use of jackfruit peel carbon (JPC) for adsorption of rhodamine-B, a basic dye from aqueous solution. *Indian J Chem Technol* 13:17–23
- Langmuir I (1916) The constitution and fundamental properties of solids and liquids. *J Am Chem Soc* 38:2221–2295
- Freundlich HMF (1906) Over the adsorption in solution. *Z Phys Chem* 57:385–471
- Murugan M, Subramanian E (2006) Studies on defluoridation of water by Tamarind seed, and unconventional biosorbent. *J Water Health* 4:453–461
- Lagergren S (1898) About the theory of so-called adsorption of soluble substances. *Kungliga Svenska Vetenskapsakademiens. Hand lingen* 24:1–39
- Ho YS, McKay G (1999) Pseudo-second order model for sorption processes. *Process Biochem* 34:451–465
- Weber WJ, Morris JC (1963) Kinetics of adsorption on carbon from solution. *J Sanit Eng Division* 31–59
- Thomas HC (1948) Chromatography: a problem in kinetics. *Ann N Y Acad Sci* 49:161–182
- Yoon YH, Nelson JH (1984) Application of gas adsorption kinetics. I. a theoretical model for respirator cartridge service life. *Am Ind Hyg Assoc J* 45:509–516
- Malkoc E, Nuhoglu Y, Abali Y (2006) Cr (VI) adsorption by waste acorn of *Quercus ithaburensis* in fixed beds: prediction of breakthrough curves. *Chem Eng J* 119:61–68
- Bhaumik M, Setshedi Maity KA, Onyango MS (2013) Chromium (VI) removal from water using fixed bed column of polypyrrole/ Fe_3O_4 nanocomposite. *Sep Purifi Technol* 69:11–19
- Chowdhury ZZ, Zain SM, Rashid AK, Rafique RF, Khalid K (2013) Breakthrough curve analysis for column dynamics sorption of Mn(II) ions from wastewater by using Mangostana garcinia peel-based granular-activated carbon. *J chem* 1–8. doi:10.1155/2013/959761
- Kalavathy MH, Miranda LR (2010) *Moringa oleifera*—a solid phase extractant for the removal of copper, nickel and zinc from aqueous solutions. *Chem Eng J* 158:188–199
- Liu L, Wan Y, Xie Y, Zhai R, Zhang B, Liu J (2012) The removal of dye from aqueous solution using alginate-halloysite nanotube beads. *Chem Eng J* 187:210–216

